

MIGE: Mutually Enhanced Multimodal Instruction-Based Image Generation and Editing

Xueyun Tian

tianxueyun23z@ict.ac.cn

State Key Laboratory of AI Safety,
Institute of Computing Technology,
Chinese Academy of Sciences
Beijing, China
University of Chinese Academy of
Sciences
Beijing, China

Wei Li

weiliucas.ict@gmail.com

State Key Laboratory of AI Safety,
Institute of Computing Technology,
Chinese Academy of Sciences
Beijing, China

Bingbing Xu

xubingbing@ict.ac.cn

State Key Laboratory of AI Safety,
Institute of Computing Technology,
Chinese Academy of Sciences
Beijing, China

Yige Yuan

yuanyige20z@ict.ac.cn

State Key Laboratory of AI Safety,
Institute of Computing Technology,
Chinese Academy of Sciences
Beijing, China
University of Chinese Academy of
Sciences
Beijing, China

Yuanzhuo Wang

wangyuanzhuo@ict.ac.cn

State Key Laboratory of AI Safety,
Institute of Computing Technology,
Chinese Academy of Sciences
Beijing, China

Huawei Shen

shenhuawei@ict.ac.cn

State Key Laboratory of AI Safety,
Institute of Computing Technology,
Chinese Academy of Sciences
Beijing, China
University of Chinese Academy of
Sciences
Beijing, China

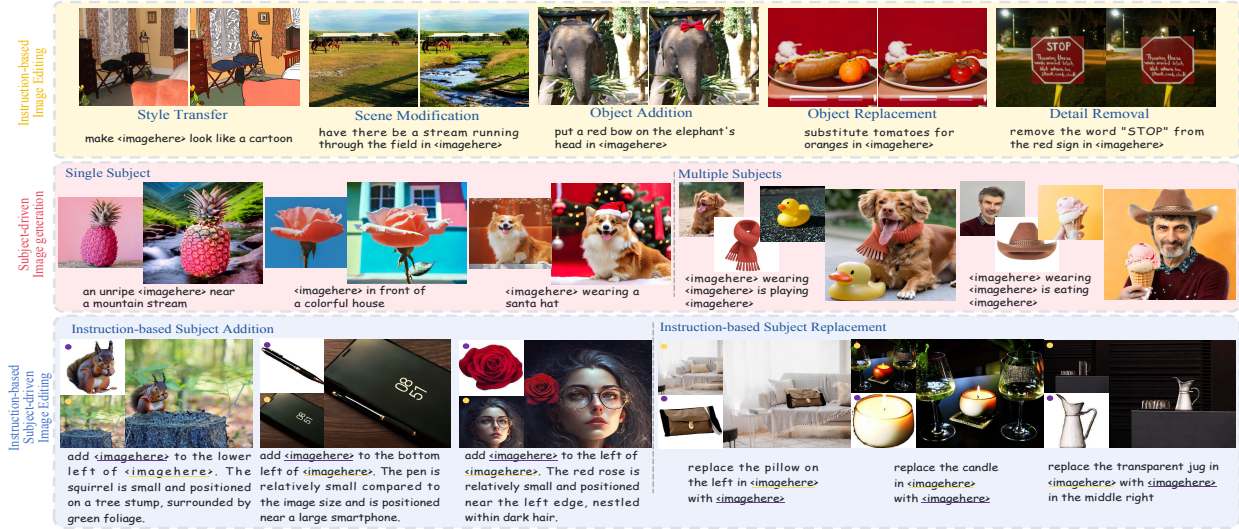


Figure 1: Demonstrating the comprehensive capabilities of MIGE, a unified framework that excels in subject-driven generation and instruction-based editing, while achieving the best performance on instruction-based subject-driven editing.

Permission to make digital or hard copies of all or part of this work for personal or classroom use is granted without fee provided that copies are not made or distributed for profit or commercial advantage and that copies bear this notice and the full citation on the first page. Copyrights for components of this work owned by others than the author(s) must be honored. Abstracting with credit is permitted. To copy otherwise, or republish, to post on servers or to redistribute to lists, requires prior specific permission and/or a fee. Request permissions from permissions@acm.org.
MM '25, Dublin, Ireland

© 2025 Copyright held by the owner/author(s). Publication rights licensed to ACM.
ACM ISBN 979-8-4007-2035-2/2025/10
<https://doi.org/10.1145/3746027.3755811>

Abstract

Despite significant progress in diffusion-based image generation, subject-driven generation and instruction-based editing remain challenging. Existing methods typically treat them separately, struggling with limited high-quality data and poor generalization. However, both tasks require capturing complex visual variations while maintaining consistency between inputs and outputs. Inspired by this, we propose MIGE, a unified framework that standardizes task

representations using multimodal instructions. It first treats subject-driven generation as creation on a blank canvas and instruction-based editing as modification of an existing image, establishing a shared input-output formulation, then introduces a novel multimodal encoder that maps free-form multimodal instructions into a unified vision-language space, integrating visual and semantic features through a feature fusion mechanism. This unification enables joint training of both tasks, providing two key advantages: (1) **Cross-Task Enhancement**: by leveraging shared visual and semantic representations, joint training improves instruction adherence and visual consistency in both subject-driven generation and instruction-based editing. (2) **Generalization**: learning in a unified format facilitates cross-task knowledge transfer, enabling MIGE to generalize to novel compositional tasks, including instruction-based subject-driven editing. Experiments show that MIGE excels in both subject-driven generation and instruction-based editing while setting a SOTA in the new task of instruction-based subject-driven editing. Code and model have been publicly available at this link.

CCS Concepts

• Computing methodologies → Image representations.

Keywords

Controllable Image Generation, Diffusion Model, Joint Training

ACM Reference Format:

Xueyun Tian, Wei Li, Bingbing Xu, Yige Yuan, Yuanzhuo Wang, and Huawei Shen. 2025. MIGE: Mutually Enhanced Multimodal Instruction-Based Image Generation and Editing. In *Proceedings of the 33rd ACM International Conference on Multimedia (MM '25)*, October 27–31, 2025, Dublin, Ireland. ACM, New York, NY, USA, 16 pages. <https://doi.org/10.1145/3746027.3755811>

1 Introduction

Recent advances in diffusion models [10, 29, 46, 50] have significantly advanced the development of customized image generation, enabling its widespread adoption in both subject-driven generation [25, 26, 31, 40, 45, 47, 51, 61, 67] and instruction-based editing [2, 12, 15, 52]. The former focuses on preserving a given subject, while the latter emphasizes flexible modifications guided by textual instructions. Their capability to generate personalized and controllable results demonstrates substantial practical value, thereby attracting growing research attention.

Existing approaches [19, 21, 31, 45] typically treat these two tasks independently and address them separately by tailoring specific input-output formats to each. However, this results in limited generalization capability and necessitates extensive training data. Specifically, subject-driven generation aims to preserve subject identity while adhering to textual instructions. Fine-tuning methods, like DreamBooth [51], require separate training for each subject during testing, which limits generalization. In contrast, zero-shot methods like KOSMOS-G [45] rely on multimodal alignment but struggle with instruction following, mainly due to the scarcity of high-quality multimodal training data, especially for multi-subject inputs. Instruction-based editing, exemplified by InstructPix2Pix [2], modifies images based on instructions. These methods require large, high-quality editing datasets to handle diverse instructions but struggle with maintaining local-to-global consistency.

The above separate processing methods can only rely on limited data and single-task optimization objectives, which hinders their ability to adapt to diverse subjects or editing requirements, and lack cross-task consistency, preventing a unified understanding of the tasks. To address these challenges, we shift our perspective from separate processing to the objectives of these two tasks. These two tasks share a fundamental principle: maintaining visual consistency between inputs and outputs while capturing variations guided by instructions. They also follow a similar input-output paradigm with complementarities: subject-driven generation emphasizes subject accuracy, while instruction-based editing manipulates images without altering irrelevant identities. These limitations and complementarities highlight the need for a unified framework that takes advantage of the strengths of both tasks to improve performance.

Inspired by the above analysis, we propose a unified framework, MIGE, which leverages Multimodal Instructions to unify subject-driven image Generation and instruction-based Editing. The vision-language representation enables substituting both entities and entire images in text prompts with their visual counterparts, allowing flexible task and instruction combinations. Structurally, we model subject-driven generation as creating an image on a blank canvas and instruction-based editing as modifying an existing image. This coherent input-output mapping simplifies the process while enabling both tasks to reinforce each other through joint training. Moreover, this integrated approach fosters emergent compositional capabilities beyond what either task can achieve alone.

Building on our unified framework, we address two critical challenges. First, for multimodal instruction encoding, existing methods [32, 35, 45] mainly rely on CLIP vision encoders [48] to extract semantic features, which is insufficient for preserving fine-grained subject details. To overcome this limitation, we propose a multimodal encoder with a feature fusion mechanism that integrates VAE [27] visual features into semantic tokens, effectively capturing both detailed visual information and semantics. Secondly, we enhance compositionality through joint training, facilitating instruction-based subject-driven editing. To further optimize performance in this complex task, we develop a novel data construction pipeline based on a Multimodal Large Language Model (MLLM). This pipeline autonomously generates diverse multimodal instructions and corresponding output images. Moreover, to address the absence of an evaluation benchmark for this new composition task, we introduce MIGEBench. This specialized benchmark evaluates compositionality in terms of subject preservation and instruction adherence, providing a comprehensive assessment of the new task.

Our experiments demonstrate that joint training under the MIGE framework enables mutual enhancement between subject-driven generation and instruction-based editing, leading to significant performance gains over training on individual tasks. As shown in Figure 2, joint training markedly improves input-output consistency across both tasks, especially in editing, with scores rising from 0.821 to 0.873. Moreover, MIGE achieves state-of-the-art results on MIGEBench, showcasing its fine-grained controllability in emerging compositional tasks. Extensive case studies (Figures 7–8) further demonstrate the ability of MIGE to generate precise and consistent outputs, highlighting its effectiveness across diverse scenarios.

In summary, our contributions include:

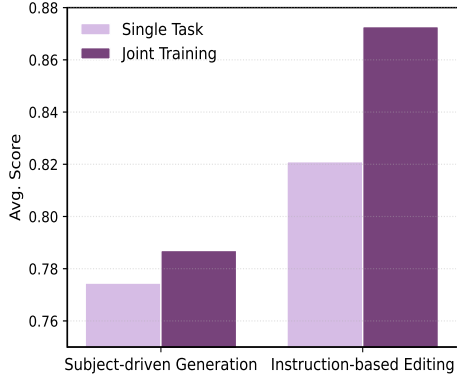


Figure 2: Joint training significantly improves input-output similarity across both tasks. We show the average DINO and CLIP-I scores for subject-driven generation and instruction-based editing under single-task and joint training.

- **Promising perspective of task mutual enhancement:** We shift our perspective from traditional separate processing to mutual enhancement. Then, we design a unified input-output format for joint training on subject-driven generation and instruction-based editing, validating that joint training enables task enhancement.
- **Novel framework for Compositional Capability:** We propose MIGE, a unified framework integrating two mainstream tasks in controllable image generation. Joint training further enables the compositional capability of instruction-based subject-driven editing. We also introduce a novel data pipeline and MIGEBench for comprehensive evaluation.
- **Strong Performance with Extensive Experiments:** Extensive results show that MIGE performs competitively on subject-driven generation and instruction-based editing, with scores rising from 0.821 to 0.873, and sets a new state-of-the-art in instruction-based subject-driven editing.

2 Related Work

In this section, we discuss the most relevant studies. A more comprehensive discussion can be found in the Supplementary Material.

Universal generative model. Unifying tasks in image generation remains challenging. Some methods [20, 39] focus on bridging image understanding and generation, such as SEED-X [13], Emu2 [54], and WeGen [22], which use autoregressive models with auxiliary diffusion modules. UnifiedMLLM [38] employs MLLMs to learn shared representations and route to task-specific models. However, these approaches either emphasize understanding over generation or rely on complex pipelines. Others aim to unify generation and editing. Pixwizard [41] uses text-only instructions and task vectors. Instruct-Imagen [19] supports multimodal inputs but performs poorly on editing. ACE [15] is limited to editing via transformer-based conditioning. OmniGen [62] cannot distinguish reference images. OmniControl [56] merges all conditions with noise, while UniReal [7] adds finer control but requires complex prompts. RealGeneral [42] enhances attention, and OnePic [57] depends on

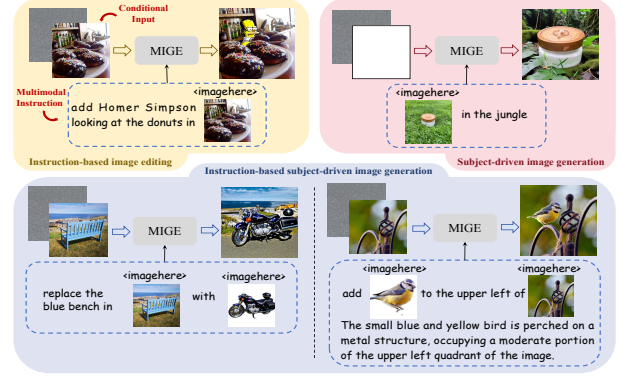


Figure 3: Demonstration of MIGE as a unified framework for processing multimodal instructions and conditional inputs across diverse scenarios.

multiple references and masks. Overall, prior work often sacrifices flexibility or generality, combining tasks without leveraging their intrinsic connections. In contrast, we propose MIGE, which jointly trains on subject-driven generation and instruction-based editing, revealing their mutual benefits.

Subject-Driven Image Editing. Subject-driven image editing enables modifications based on a user-specified subject, typically including addition or replacement. Existing methods often rely on multiple reference images or precise cues. DreamEdit [34] and DreamMix [66] require multiple images for fine-tuning and iterative inpainting. PBE [65] uses compressed reference embeddings, while TIGIC [33] embeds subjects into predefined backgrounds. MADD [16] supports diverse controls via masks or coordinates. AnyDoor [6], AnyEdit [69], MimicBrush [5] and BlobCtrl [37] require masks or additional range blobs. FreeEdit [17] is limited to instruction templates and class-aware features. Overall, these approaches depend on detailed inputs and lack flexibility in handling diverse instructions for controllable generation.

3 Method

In this section, we first shift our view from separate training to mutual enhancement. Guided by this new perspective, we first introduce the unified framework MIGE, followed by details of the architecture design and joint training approach.

3.1 Unified framework MIGE

Current methods treat subject-driven generation and instruction-based image editing separately, hindering performance due to data limitations and poor generalization. Since both aim to preserve visual consistency while incorporating instructed changes, unifying them allows mutual improvement. Joint training on diverse data enhances subject preservation and instruction following beyond the capabilities of individual task-specific models.

Therefore, we propose MIGE to unify the two tasks for joint training. By using multimodal instructions as a unified task representation, it supports flexible combinations and provides multimodal guidance. Additionally, we use conditional input to structurally

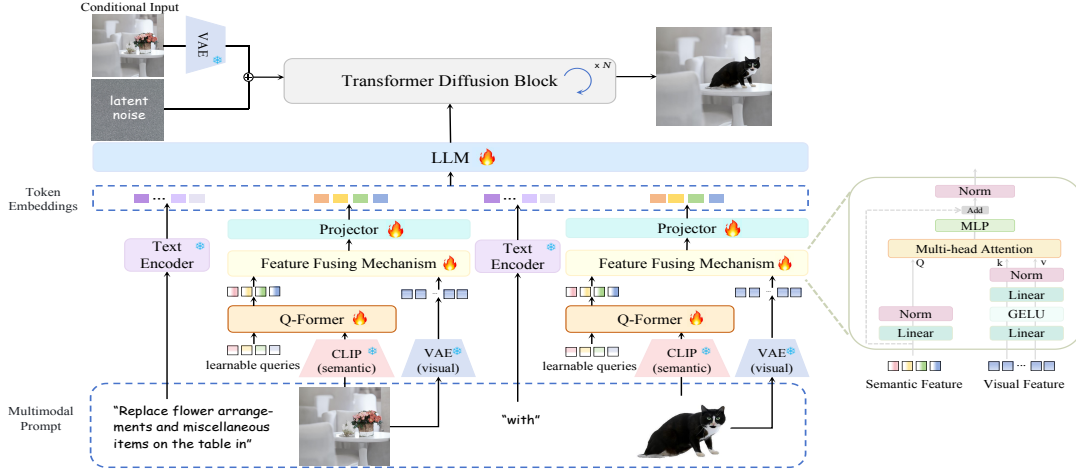


Figure 4: Overall framework of MIGE. MIGE consists of two components: a multimodal encoder for processing multimodal instructions and a transformer-based diffusion model for modeling input-output relationships. The encoder incorporates a feature fusion mechanism to integrate visual and semantic features from reference image.

unify the tasks, enhancing visual consistency. Their combination not only provides rich visual and instructional information but also naturally represents different tasks. We demonstrate the input-output format of MIGE in Figure 3.

3.1.1 Unified Multimodal Instruction. To enable joint training across multiple tasks, a unified task representation is essential. We introduce multimodal instructions composed of interleaved images and text, which provide both visual references and textual guidance for various controllable generation tasks. As shown in Figure 3, “<imagehere>” serves as a placeholder, sequentially replaced by input images, which can be the reference subject or the entire scene, complementing the semantics to form interleaved expressions. This unified approach effectively accommodates subject-driven generation and instruction-based editing while remaining extensible to the more complex combination task.

3.1.2 Unified Conditional Input. We design a unified conditional input format to distinguish tasks while enabling shared capabilities. As shown in Figure 3, conditional inputs vary across tasks. For instruction-based editing, the VAE-encoded source image is used to preserve fine details of the original image, inform the model to edit only the target region, as done in prior editing methods [2, 70]. To standardize the input format, we concatenate an all-zero tensor for subject-driven generation to indicate generation from scratch with visual constraints from the multimodal instruction. This design unifies the input format, ensures input-output consistency, and facilitates extensibility to new tasks within a unified framework.

3.2 Architecture

The architecture of MIGE, as shown in Figure 4, consists of two main components: a multimodal encoder for processing multimodal instructions and a transformer-based diffusion model [46] for modeling input-output relationships. The diffusion model takes concatenated latent noise and conditional input along the channel dimension as input, performing controllable generation under the

control of multimodal conditions. To further enhance the integration of visual and semantic information from the reference image, we introduce a novel feature fusion mechanism in the encoder.

3.2.1 Multimodal Encoder. To map the multimodal instructions into a unified vision-language semantic space, we design a multimodal encoder comprising a Large Language Model (LLM) and an image feature encoding component, which includes a pretrained VAE encoder [27] for visual feature extraction, a pretrained ViT from EVA-CLIP [11] for semantic feature extraction, a Q-Former [32], and a linear projection layer. Each image is represented by 32 tokens, which are then encoded by the LLM alongside text tokens to form a unified multimodal condition.

Prior works [31, 35, 45] focus on extracting semantics from reference images but lack the fine-grained details needed to preserve subject-specific features. To address this, we propose a feature fusion mechanism that combines the strengths of different visual encoders. ViT serves as a semantic feature extractor, while a VAE encoder acts as a visual feature extractor, leveraging its ability to compress and reconstruct images. As shown in Figure 4, we use the ViT semantic features compressed by the Q-Former, denoted as f_s , as guidance to adaptively incorporate the visual features f_v extracted by the VAE. Inspired by TokenPacker [36], we represent rich features with fewer tokens, and apply ReLU [14] to enhance stability. The fusion mechanism is expressed as: $f_{img} = f_s + \text{MLP}(\text{Attn}(f_s, f_v))$ where $\text{Attn}(f_s, f_v) = \frac{Q(f_s) \cdot K(f_v)}{\sqrt{d}} V(f_v)$. Here d denotes the output dimension of the features, Q is a linear layer, and both K and V are two-layer networks, where $K(\cdot) = V(\cdot) = \text{Linear}(\text{GELU}(\text{Linear}(\cdot)))$.

This fusion mechanism captures both semantic and visual information without introducing extra image tokens. The multimodal encoder compresses each image into 32 fused tokens, which replace the “<imagehere>” placeholder in the interleaved instruction. The LLM then encodes the entire prompt into a unified vision-language representation to guide the diffusion model.

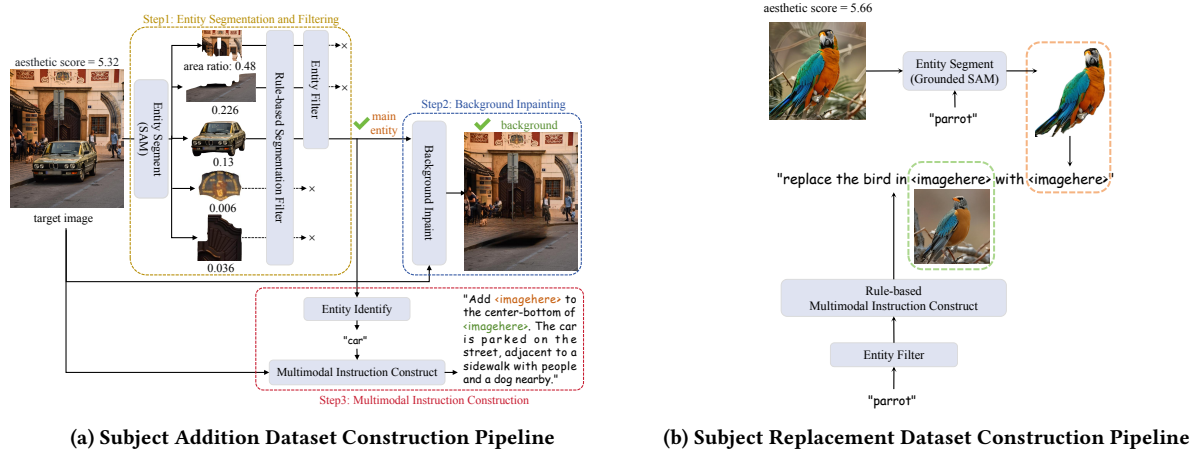


Figure 5: Data construction pipelines for instruction-based subject-driven image editing.

3.3 Joint Training

Multimodal instructions and conditional input unify task representation and input-output formats, enabling joint training. We fine-tune MIGE on data from all tasks to enhance cross-task synergy. Except for the two image encoders, all parameters are jointly trained to align the conditional space of the diffusion model with the multimodal encoder, as shown in Figure 4. This approach improves task coordination and consistency across modalities.

3.3.1 Data Construction. Joint training enables multi-task learning, balancing subject preservation and instruction, followed by modeling task relationships. We create a multi-task dataset for joint multimodal instruction tuning, covering subject-driven image generation, instruction-based image editing, and instruction-based subject-driven image generation.

For subject-driven image generation, we follow the data construction methods of KOSMOS-G [45] and UNIMO-G [35], using an LLM to extract entities from captions, which are then fed into Grounded SAM [49] for segmentation. Subjects200k dataset from OmniControl [56] is also incorporated for better object preservation. For instruction-based editing, we filter existing datasets and use a rule-based strategy to construct multimodal instructions.

Instruction-based subject-driven image generation is an emerging task involving two subtasks: instruction-based subject addition and subject replacement, which allows users to add or replace a specified subject in an image using multimodal instructions. However, there is no sufficient dataset available for this task.

For instruction-based subject addition, we propose a pipeline inspired by SAM-FB [16], as shown in Figure 5a. Starting with the SA-1B [28] dataset, we construct the source image and a multimodal instruction for input-output pairs. We use SAM [28] to segment annotated entities, filter and retain the main subject using an MLLM, inpaint the remaining parts to create the background, and then combine the subject name with the target image to generate the multimodal instruction via GPT-4o [24]. Due to resource limitations, we process a part of the SA-1B dataset and obtain about 200k samples, but the pipeline can be scaled to generate more. For instruction-based subject replacement, we filter from existing

editing data, use Grounded SAM for subject segmentation, and construct multimodal instructions to form input-output pairs, as shown in Figure 5b. We also introduce virtual try-on data constructed using IDM-VTON [8], resulting in approximately 110k samples. More details on training data construction are in Supplementary Material.

4 Experiments

In this section, we present experimental results on three tasks, followed by analysis of the joint training strategy and framework design. For subject-driven image generation, we compare our method with both task-specific models using MLLMs as encoders and recent unified frameworks. For instruction-based image editing, we similarly compare against both task-specific and unified models, including SmartEdit [21] and ml-MGIE [12], which also use MLLMs. For instruction-based subject-driven image editing, given the lack of instruction-only baselines, we additionally evaluate mask-dependent methods using masks from MIGEBench.

4.1 Implementation Details

MIGE includes a conditional diffusion model and a multimodal encoder. Our design allows flexible selection of various diffusion models, and we initialize with PIXART- α [4] pretrained at a 512×512 resolution. The multimodal encoder consists of a pretrained Flan-T5-XXL [9] as LLM for initialization and an image encoding component. This includes query tokens, Q-Former, and a projector, all initialized with a BLIP-2 [32] checkpoint (pretrain_flan5xxl). The frozen VAE encoder, used as the visual feature extractor, is the same as the one in the diffusion model. During training, we sample instruction-based subject addition and subject replacement data in a 1:1 ratio. Separately, subject-driven editing and instruction-based editing data are also sampled in a 1:1 ratio. A training strategy is employed with a 5% probability of dropping either the conditional input or the multimodal condition, and an additional 5% chance of dropping both, enabling classifier-free guidance during inference.

4.2 Evaluation Results

As a unified model, MIGE demonstrates exceptional performance across various image generation and editing tasks, even outperforming existing task-specific models. MIGE achieves strong performance in subject-driven generation and instruction-based editing, and shows promising results on instruction-based subject-driven image generation. Detailed results are in Supplementary Material.

4.2.1 Instruction-based Image Editing. Instruction-based image editing allows users to modify a source image using free-form multimodal instructions, such as adding, removing, or altering objects and styles. Table 1 reports results on Emu Edit and MagicBrush [70]. DINO and CLIP-I assess similarity to the source image, CLIP-T evaluates alignment with the target caption, $CLIP_{dir}$ measures consistency between text and image embedding changes, and L1/L2 capture pixel-level differences.

As shown in Table 1, MIGE achieves the highest CLIP-T and outperforms all task-specific models on $CLIP_{dir}$, indicating stronger instruction following. On MagicBrush, it surpasses all universal models across almost all metrics, with the best DINO, CLIP-I, CLIP-T, and lowest L1/L2, demonstrating superior instruction fidelity and detail preservation. This capability is further illustrated in Figure 6, where MIGE is the only model that accurately follows the instruction to add a Daffy Duck image to the red suitcase without altering other unrelated areas. Compared to ml-MGIE, which also uses a MLLM as an encoder, MIGE better preserves input-output consistency and avoids altering irrelevant backgrounds.

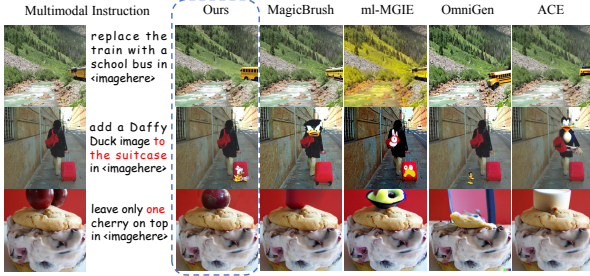


Figure 6: Qualitative comparison for instruction-based image editing. MIGE demonstrates superior editing accuracy and instruction understanding.

4.2.2 Subject-driven Image Generation. Generating images that satisfy both image and text constraints from a multimodal prompt is challenging. We compare MIGE with three task-specific methods using MLLMs as encoders and three universal models on DreamBench [51]. DINO and CLIP-I measure subject fidelity, while CLIP-T assesses instruction adherence. As shown in Table 2, MIGE surpasses all unified models in subject preservation ability, as evidenced by the highest DINO and CLIP-I scores, with the DINO score even outperforming task-specific models. Examples in Figure 7 further highlight MIGE’s ability to effectively preserve the identity of each object in multi-object scenarios and combine them based on instructions, demonstrating that our multimodal encoder effectively captures both semantic and visual features simultaneously.

4.2.3 Instruction-based Subject-driven Image Editing.



Figure 7: Qualitative comparison for subject-driven image generation. MIGE exhibits superior subject preservation, even in multi-subject scenarios.

Benchmark Construction. Instruction-based subject-driven image editing is a novel task. Existing methods rely on masks or positional cues for editing [34, 66] but lack support for instruction-only editing. The AnyEdit-Test Benchmark [69] supports few instruction templates and evaluates only one type of object editing based on automatically extracted masks. Current benchmarks [6, 65] for subject addition and replacement separately evaluate foreground and background similarities without providing a complete edited image as ground truth, making them unsuitable for this task.

To address these issues, we manually construct MIGEBench, a benchmark consisting of 1,000 test samples: 500 for instruction-based subject addition and 500 for subject replacement. More details can be found in the Supplementary Material.

Evaluation Results. Our evaluation focuses on editing ability and subject preservation. DINO and CLIP-I measure the similarity of the generated image to the ground truth, while CLIP-T evaluates alignment with the target caption, indicating editing ability. Subject preservation is evaluated by extracting the edited subject via Grounded SAM [49] and comparing it to the input subject image using DINO and CLIP-I. This separates the evaluation of image-level editing from subject-level feature preservation. Methods that do not support instruction-based editing use masks provided in MIGEBench during testing.

Quantitative comparisons with other methods are shown in Tables 3a and 3b. We compute the DINO, CLIP-I, and CLIP-T scores between the input image and the ground truth. The first row of the table (denoted as "I-O sim") provides a baseline for evaluating the effectiveness of editing ability. Mask-dependent models can easily preserve the edit-unrelated regions, but MIGE still outperforms all methods, highlighting the effectiveness of conditional inputs and MIGE’s precise understanding of instructions. The CLIP-T score measures instruction adherence in mask-free models. MIGE significantly outperforms OmniGen in both tasks, demonstrating

Table 1: Quantitative results on the Emu Edit and MagicBrush test sets. MIGE outperforms other universal models on MagicBrush, demonstrating superior instruction alignment and detail preservation.

		Emu Edit Test set						MagicBrush Test set					
	Methods	DINO ↑	CLIP-I ↑	CLIP-T ↑	CLIP _{dir} ↑	L1 ↓	L2 ↓	DINO ↑	CLIP-I ↑	CLIP-T ↑	CLIP _{dir} ↑	L1 ↓	L2 ↓
Task-specific Models	InstructPix2Pix [2]	0.759	0.831	0.288	0.086	0.122	0.036	0.763	0.843	0.289	0.105	0.097	0.028
	MagicBrush [70]	0.800	0.857	0.295	0.102	0.085	0.027	0.847	0.888	0.304	0.127	0.062	0.018
	UltraEdit [71]	0.862	<u>0.875</u>	<u>0.301</u>	0.100	0.050	0.008	<u>0.879</u>	0.897	<u>0.305</u>	<u>0.119</u>	0.042	0.006
	SmartEdit [21]	0.752	0.830	0.290	0.100	0.129	0.055	0.821	0.879	0.301	0.122	0.084	0.033
	ml-MGIE [12]	0.779	0.843	0.276	0.040	0.101	0.034	0.751	0.844	0.274	0.039	0.102	0.034
Unified Models	PixWizard [41]	0.824	0.862	0.288	0.066	0.105	0.038	0.865	0.897	0.289	0.054	0.073	0.023
	ACE [15]	<u>0.847</u>	0.877	0.299	0.104	<u>0.079</u>	0.028	0.856	<u>0.899</u>	0.304	0.127	0.065	0.023
	OmniGen [62]	0.766	0.819	0.299	0.123	0.160	0.065	0.821	<u>0.863</u>	0.289	0.087	0.116	0.045
	OneDiff [30]	0.728	0.819	0.285	0.082	0.136	0.060	0.742	0.840	0.295	0.107	0.128	0.052
	MIGE (ours)	0.832	0.865	0.306	<u>0.114</u>	0.088	<u>0.027</u>	0.889	0.905	0.306	<u>0.119</u>	<u>0.055</u>	<u>0.013</u>
	/only_edit data	0.785	0.841	0.302	0.104	0.117	0.046	0.796	0.862	0.300	0.111	0.094	0.036
	/wo_VAE feature	0.799	0.846	0.300	0.098	0.103	0.035	0.811	0.868	0.299	0.105	0.098	0.036
	/wo_multimodal instruction	0.592	0.723	0.280	0.113	0.177	0.074	0.548	0.714	0.277	0.135	0.170	0.066

Table 2: Quantitative results for subject-driven image generation on DreamBench. Results with * denote our reproduction. MIGE outperforms universal models in subject preservation and is competitive with task-specific models.

	Methods	DINO ↑	CLIP-I ↑	CLIP-T ↑
Task-specific Models	BLIP-Diffusion [31]	0.670	0.805	0.302
	KOSMOS-G [45]	0.694	0.847	0.287
	UNIMO-G [35]	0.668	<u>0.841</u>	0.329
Unified Models	OmniGen * [62]	<u>0.711</u>	0.800	0.312
	UniReal [7]	0.702	0.806	<u>0.326</u>
	OneDiffusion * [30]	0.582	0.750	0.240
	MIGE (ours)	0.744	0.830	0.293
	/only_subject data	0.726	0.823	0.289
	/wo_VAE feature	0.741	0.828	0.287

the advantage of our unified approach. MIGE also achieves the best performance on subject preservation in both tasks. As shown in Figure 8, MIGE successfully understands the task of replacing a bird with an owl, rather than simply overlaying or adding an owl, demonstrating the effectiveness of the multimodal encoder which simultaneously encoding the semantic and visual information of the reference image.

4.3 Further Analysis

4.3.1 Effectiveness of Joint Training. To assess the effectiveness of joint training, we train models separately on individual datasets (denoted as “only_subject data,” “only_edit data,” and “only_compositional data”) and compare their performance with the jointly trained model. The results in Tables 1, 2 and 3 show that joint training leads to consistent improvements across all metrics, demonstrating that subject-driven generation and instruction-based editing reinforce each other. As shown in Table 3, joint training also enhances the performance of the compositional new task, further highlighting its overall benefits. These findings emphasize both the effectiveness and necessity of joint training. In conclusion, joint training of subject-driven generation and instruction-based editing within our unified framework not only boosts compositional capability but also improves the performance of each individual task. This validates our motivation and provides further theoretical support for unified models for multiple tasks.

4.3.2 Effectiveness of Feature Fusing. MIGE employs a feature fusion mechanism in the multimodal encoder to integrate semantic features from ViT and visual features from VAE. As shown in Table 2, Table 1 and Table 3, compared to the model without VAE features (denoted as “wo_VAE feature”), incorporating VAE features significantly improves detail preservation in reference images, benefiting both subject-driven image generation and instruction-based image editing. This is particularly evident in the improved CLIP-I and DINO scores and the significant reduction in L1 and L2 metrics, demonstrating that the inclusion of additional visual features helps maintain consistency between the input and output.

4.3.3 Effectiveness of Instruction-based Subject-driven Image Editing Dataset. Joint training of subject-driven image generation and instruction-based image editing enables generalization to instruction-based subject-driven image editing (denoted as “subject data + edit data”). To enhance the capability of MIGE in this new task, particularly in understanding spatial terms and size descriptions, we constructed a task-specific dataset for joint training. As shown in Table 3a and Table 3b, the task-specific data significantly improved the model’s overall abilities. This demonstrates the effectiveness of our constructed dataset, and the proposed data generation pipeline serves as a valuable reference for future dataset construction.

4.3.4 Effectiveness of Multimodal Instruction. Existing instruction-based editing works [2, 52, 70] typically use text instructions as the conditional input, while we extend this to multimodal instructions. To measure the benefit of multimodal instructions, we trained the model with text-only editing instructions for comparison. As a unified model, MIGE demonstrates exceptional performance across various image generation and editing tasks, even outperforming existing task-specific models. As shown in Table 1, using multimodal instructions consistently improves performance over text-only instructions (denoted as “wo_multimodal instruction”). This enhances input-output consistency and instruction-following ability in multi-task training. The significant improvement in the L1 and L2 metrics indicates finer control over images and more accurate edits. While text-only instructions provide the necessary changes, the high CLIP_{dir} score and lower values in other metrics show that multimodal instructions add visual context, enabling more precise and faithful modifications. For more qualitative results, see Supplementary Material.

Table 3: Quantitative results on instruction-based subject-driven editing. Methods marked with a cross in the instruction column use masks, while the others generate images using multimodal instructions. Overall, MIGE significantly outperforms others in both tasks, showcasing superior editing and subject preservation abilities.

(a) Results on instruction-based subject replacement.							(b) Results on instruction-based subject addition.						
Methods		Editing			Subject Preserving		Methods		Editing			Subject Preserving	
		DINO ↑	CLIP-I ↑	CLIP-T ↑	DINO ↑	CLIP-I ↑			DINO ↑	CLIP-I ↑	CLIP-T ↑	DINO ↑	CLIP-I ↑
<i>I-O sim</i>		0.668	0.842	0.271			<i>I-O sim</i>		0.783	0.903	0.295		
Mask-dependent Models	PBE [65]	0.810	0.885	0.304	0.521	0.792	Mask-dependent Models	PBE [65]	0.843	0.908	0.321	0.495	0.794
	AnyDoor [6]	0.817	0.890	0.307	0.551	0.789		AnyDoor [6]	0.863	0.930	0.324	0.533	0.799
	TIGIC [33]	0.789	0.874	0.313	0.453	0.744		TIGIC [33]	0.840	0.901	0.325	0.455	0.753
	MADD [16]	0.736	0.852	0.284	0.446	0.742		MADD [16]	<u>0.885</u>	<u>0.930</u>	0.316	0.519	0.785
Mask-free Models	OmniGen [62]	0.802	0.868	0.296	0.580	0.792	Mask-free Models	OmniGen [62]	0.791	0.870	0.312	<u>0.605</u>	<u>0.814</u>
	MIGE(ours)	0.863	0.909	<u>0.307</u>	0.652	0.834		MIGE(ours)	0.909	0.940	<u>0.322</u>	0.638	0.838
	/subject data + edit data	0.789	0.873	0.299	0.503	0.764		/subject data + edit data	0.807	0.895	0.304	0.309	0.683
	/only_compositional data	0.780	0.860	0.303	0.585	0.808		/only_compositional data	0.879	0.928	0.324	0.577	0.820
/wo_VAE feature		0.852	0.900	0.308	0.633	0.819	/wo_VAE feature		0.902	0.934	0.322	0.633	0.831

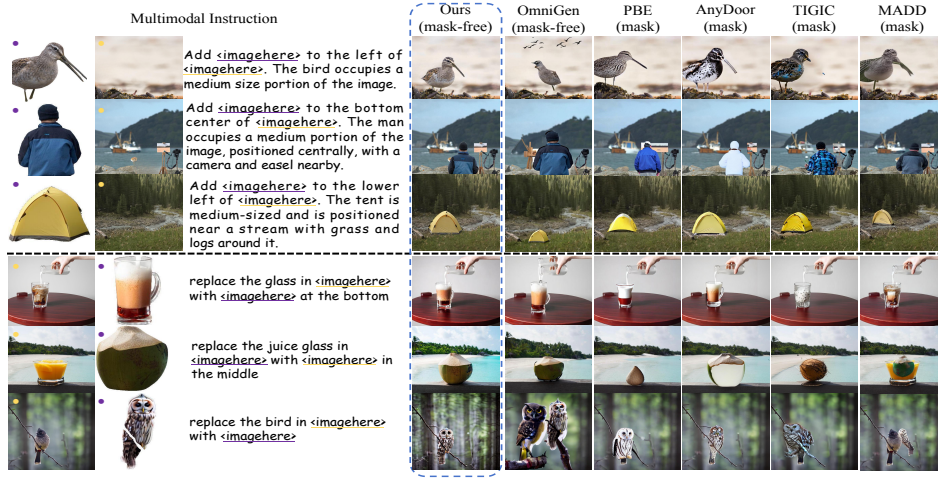


Figure 8: Qualitative results on the benchmark for the subject addition and subject replacement. The upper section compares subject addition results, while the lower section compares subject replacement. During testing, the <imagehere> placeholder in the multimodal instruction is replaced according to the image sequence. MIGE demonstrates flexibility in editing and excels in subject preservation ability and input-output consistency.

4.3.5 Comparison of Data Volume. Task-specific models treat tasks separately and typically require large amounts of high-quality data. In contrast, by exploiting the relationships between tasks and the unified structure, MIGE achieves excellent results with minimal data through joint training. As shown in Table 4, MIGE demonstrates that both the model structure and joint training are key to achieving this performance with minimal data, using fewer data than task-specific models and other unified models.

5 Conclusion

We present MIGE, a unified framework that combines subject-driven generation and instruction-based editing, leveraging multimodal instructions and conditional input for joint training that enhances task synergy. Joint training also unlocks new capabilities like instruction-based subject-driven image editing. We introduce pipelines for this new task to construct training data and MIGEBench for evaluation. Our experiments show that joint training leads to significant

Table 4: Comparison of Data Volume Across Methods

Methods		Data Volume
Task-specific Models	MADD [16]	3M
	PBE [65]	16M
	KOSMOS-G [45]	3159.3M
	UNIMO-G [35]	304.3M
Unified Models	PixWizard [41]	30M
	UniReal [7]	100M
	ACE [15]	700M
	Omnigen [62]	326.06M
	MIGE (ours)	2.28M

enhancement in subject fidelity and instruction adherence, demonstrating the effectiveness of unifying these tasks. This integration enhances controllability and offers promising directions for future multimodal image generation and editing.

6 Supplementary Material

A Qualitative Comparison

We conduct a qualitative comparison to assess the visual performance and effectiveness of MIGE. Figure 14 presents a range of cases on each task to showcase the generation results of MIGE, demonstrating its ability to handle diverse inputs and produce high-quality outputs. This comparison highlights the strengths of MIGE and the benefit of joint training, offering valuable insights into its potential for real-world applications.

B Related Work

B.1 Subject-Driven Image Generation

Subject-driven generation focuses on preserving given subject features while generating new images. DreamBooth [51] fine-tunes the full model, leading to high resource costs. IP-Adapter [67] trains lightweight attention layers, struggles with prompt-image balance. Methods like Blip-Diffusion [31] use embeddings to condition generation, yet face challenges in subject preservation and generalization. KOSMOS-G [45] and UNIMO-G [35] leverage Multimodal Large Language Models (MLLMs) as flexible encoders, but require large datasets for task-specific adaptation and lack robust instruction-following ability, limiting transferability.

B.2 Instruction-based Image Editing

Instruction-based editing modifies images based on instructions, offering greater flexibility than caption-driven methods. Inst-inpaint [68] and EraseDraw [3] focus on object-level edits. InstructPix2Pix [2], EmuEdit [52], and MagicBrush [70] enable diverse edits via large-scale data. AnyEdit [69], FireEdit [72], and TF-TI2I [18] introduce task-aware routing, region prompts, or fixed templates. Recent works like InsightEdit [63], MGIE [12], and SmartEdit [21] leverage MLLMs to enhance instruction understanding. However, maintaining input-output consistency remains challenging.

C Dataset Construction

To enable joint training of MIGE, we designed a series of pipelines for data construction and processing. Our dataset includes three tasks: subject-driven image generation, instruction-based image editing, and instruction-based subject-driven image editing. The proportions of the training data are shown in Figure 9. In this section, we will detail the pipelines for processing each data component and other related details.

C.1 Subject-driven Image Generation Data Construction

We construct multimodal instruction-image pairs by replacing entities in image captions with corresponding entity images. The dataset combines BLIP3-GROUNDING-50M [64] and internal sources. For the former, we filter out low-quality pairs with CLIP-T scores below 0.255 and retain entities with bounding boxes sized between 0.05 and 0.8. Entities are segmented using SAM [28], and pairs with low CLIP-T scores between the prompt "a photo of [entity]" and the segmented image are removed. For internal data, we adopt the KOSMOS-G's pipeline, using MPT-7B-Instruct [58] to extract

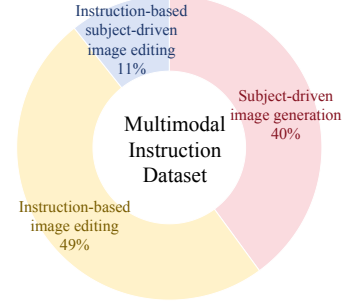


Figure 9: Composition of training data.

entities. Entity images are obtained via Grounded SAM [49], and filtered by a CLIP-T score threshold of 0.255 and a size ratio between 0.1 and 0.85. To enhance subject fidelity, we further include 112,846 samples from subject200k, following OminiControl [56].

C.2 Instruction-based Image Editing Data Construction

Previous works on instruction-based editing relied solely on text, covering object-level additions, deletions, modifications, and global changes in background or style. We integrated data from Instruct-Pix2Pix [2], UltraEdit [71], MagicBrush [70], SEED-Data-Edit [13], GIER [53], and HQ-Edit [23], filtering out instances with target image aesthetic scores above 5.5. To enhance multimodal instruction alignment, we reformulated text-based instructions based on task type. Specifically, for instructions containing phrases like "in the image" or "to the image," we replaced them with "in-<imagehere>" or "to-<imagehere>." For others, we appended "of-<imagehere>" for global edits or "in-<imagehere>" for localized modifications.

C.3 Instruction-based Subject-driven Image Editing Data Construction

For subject addition, inspired by SAM-FB [16], we construct background images, foreground entities, and multimodal instructions, as shown in Figure 5a. We filter SA-1B [28] images with aesthetic scores above 5 and select entities with a foreground-to-image ratio between 0.1 and 0.5. Qwen2-VL-7B [60] verifies entity completeness. The selected entities serve as foregrounds, and backgrounds are inpainted using LAMA [55]. Foreground-related text is extracted with Qwen2-VL-7B, and multimodal instructions are generated via GPT-4o [24]. Due to resource constraints, we process the first 500,000 SA-1B samples, yielding 193,247 multimodal instruction-foreground-background pairs.

For subject replacement, we construct foreground entities and multimodal instructions, as shown in Figure 5b. SEED-Data-Edit's part1-unsplash is filtered to retain replace-task samples with annotation match scores above 0.3 and aesthetic scores above 5.5. Qwen2.5-14B-Instruct [59] verifies the main entity. The target entity is replaced with <imagehere> to form the multimodal prompt. Grounded SAM segments entities based on annotations, resulting in 79,693 multimodal instruction-replace entity-source image-target

image pairs. We also include 34,947 virtual try-on samples generated using IDM-VTON [8].

D Prompts

LLMs and MLLMs are essential to our data and benchmark construction, with all prompts listed in Table 6 to Table 9.

E Implementation Details

E.1 Training Details

MIGE includes a conditional diffusion model and a multimodal encoder. The diffusion model is initialized from the PIXART- α checkpoint pretrained at a 512×512 resolution. Parameters introduced for handling conditional inputs are initialized to zero. The multimodal encoder consists of a pretrained Flan-T5-XXL [9] as the LLM for initialization, and an image encoding component. This image encoder includes query tokens, Q-Former, and a projector, all initialized from the BLIP-2 [32] checkpoint, with a frozen pretrained CLIP. The frozen VAE encoder, which acts as the visual feature extractor, is the same as the one in the diffusion model. Additionally, a zero-initialized MLP layer is introduced in the feature fusing mechanism for progressive visual feature integration.

MIGE is trained on our multi-task dataset using the AdamW optimizer [44] with a weight decay of 0.03 and a learning rate of $1e-5$ for 18 epochs on 48 H20 GPUs, totaling six days of training with a batch size of 960 (20 per GPU).

E.2 Evaluation Details

We evaluated the subject-driven generation capability of MIGE on DreamBench, which contains 750 prompts covering 30 subjects. For each prompt, four images were generated using seeds 0, 1, 2, and 3, resulting in 3,000 images. Following KOSMOS-G, we selected one image per prompt. Then we use the extracted subject from Grounded SAM as input, aligning with the training process. Subject fidelity was assessed using DINO and CLIP-I, while CLIP-T measured adherence to multimodal instructions.

For instruction-based editing evaluation, the Emu Edit benchmark contains known issues, including incorrect image-caption pairs and duplicate source-target captions. Prior works have handled these inconsistencies differently, leading to incomparable results. Therefore, we reimplemented all currently available open-source methods on both test sets using a fixed random seed (seed=0) for consistency. Consequently, CLIP-I, L1, and DINO were computed on 3,589 Emu Edit test samples, while CLIP- $_{dir}$ and CLIP-T were evaluated on 2,899 samples after removing problematic data.

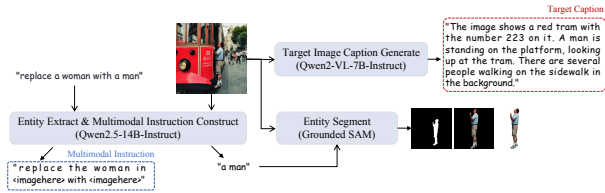


Figure 10: The pipeline of benchmark construction.

F Benchmark Construction

Instruction-based subject-driven image editing is a novel task lacking evaluation benchmarks. Previous works [34, 66] did not support variety of instructions and lacked ground truth target images. To address this, we designed a benchmark construction pipeline with multiple manual inspections to ensure image and caption quality.

As shown in Figure 10, we first filter valid editing pairs using a Gradio [1] interface, as shown in Figure 11. Then, Qwen2.5-14B-Instruct extracts entity names and constructs multimodal instructions. After manually reviewing object names, we use Grounding DINO [43] for bounding boxes and SAM for segmentation. Cropped entities are saved with black and white backgrounds for diverse test scenarios. Prompts are detailed in Supplementary Material D.

For evaluation, Qwen2-VL-7B generates captions comparing generated and ground truth images, followed by manual reviews to remove unrecognized entities and correct inaccuracies. The final benchmark includes 500 samples each for subject addition and replacement. By avoiding artifacts from inpainting and incorporating multiple manual reviews, we ensure high-quality data. Figure 12 and Figure 13 showcase some example benchmark pairs.

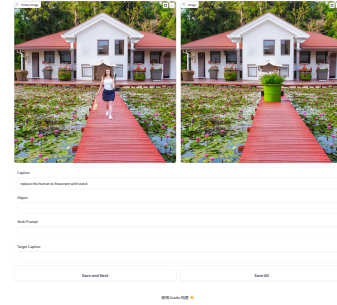


Figure 11: The annotation interface for benchmarks built with Gradio.

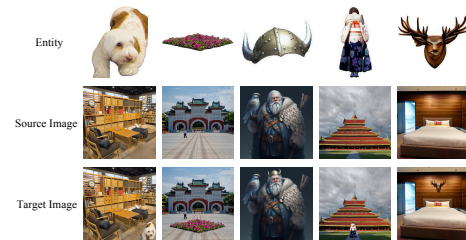


Figure 12: Subject addition examples in our benchmark.

Our benchmark, MIGEBench, is constructed based on SEED-Data-Edit, which is diversity. The benchmark covers a total of 565 distinct subjects. For the subject-replacement subset, the data is distributed across 10 major, well-balanced categories, as shown in 5. This hierarchical and balanced structure ensures a high degree of diversity throughout the MIGEBench dataset.

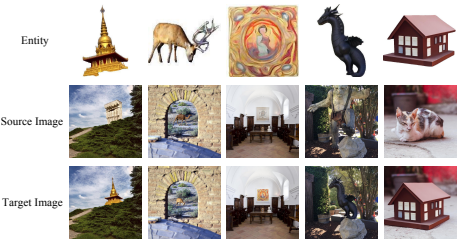


Figure 13: Subject replacement examples in our benchmark.

Table 5: Category-wise Statistics of MIGEBench

Category	Subject Replacement	Subject Addition
Animals	62	77
People	60	66
Vehicles	40	52
Buildings & Structures	27	50
Plants & Nature	30	33
Household & Man-made Objects	88	91
Art & Decor	54	47
Food & Drink	23	8
Clothing & Accessories	31	24
Other	85	52
Total	500	500

Table 6: Prompt design for subject completeness evaluation in an image. The model should identify whether the subject is complete, not abstract elements.

<i>Prompt for Qwen2-VL-7B to determine the completeness of subject in the image</i>
Prompt: Determine if the subject in the image is complete. If it is complete and not an abstract object such as background, grass, sky, tree, stone, or part of another item, please return True. Otherwise, return False.

Table 7: Prompt design for GPT-4o to generate multimodal instruction for subject addition training data.

<i>Prompt for GPT-4o to generate multimodal instruction</i>
Prompt: The object is {object_name}. It is located in a bounding box with coordinates ({x}, {y}, {w}, {h}) on an image of size {width}x{height}. Describe its size, relative position, and relation to surrounding objects. Avoid describing the overall scene or unrelated elements. Your response should start with “Add <imagehere> to the [position] of <imagehere>”. (The first <imagehere> indicates the object and the second indicates the image.) Keep the <imagehere> symbol in the first sentence in your reply. Answer briefly in two sentences:

Table 8: Prompt design for determining if an edit instruction pertains to the main subject of the image. The model evaluates whether the instruction relates to humans, animals, or other environmental features.

<i>Prompt for Qwen2.5-14B-Instruct to determine whether an edit instruction pertains to the main subject of an image</i>
Prompt: You are an assistant that determines whether an edit instruction pertains to the main subject of an image. The main subject refers to humans or animals only. If the edit instruction is related to the main subject, respond with 'yes'. If it pertains to background, large areas of vegetation, or environmental information, respond with 'no'. Here are some examples: 1. replace the grass with sand → no 2. replace the trees with palm trees → no 3. replace the dirt road with a cobblestone path → no 4. replace the bird with a parrot → yes Now, analyze the following instruction and respond accordingly: {instruction}

Table 9: Prompt designs for extracting and modifying edit instructions based on either replacement or addition of subjects.

<i>Prompt for extracting the main subject and modifying the edit instruction</i>
<p>Prompt 1: Replace Examples</p> <p>You are an assistant that determines the main subject of an edit instruction and outputs the extracted main subject along with a modified prompt.</p> <p>Given an edit instruction like “replace X with Y”:</p> <ul style="list-style-type: none"> - Extract “Y” (the replacement subject). - Output the extracted subject. - Modify the instruction by replacing “Y” with <imagehere> in the original prompt and output the new instruction. <p>Examples:</p> <ol style="list-style-type: none"> 1. replace one woman with a man → Output: a man, replace one woman with <imagehere> 2. replace the castle with another castle → Output: castle, replace the castle with <imagehere> 3. replace the desk with a white one in the bottom middle → Output: desk, replace the desk with <imagehere> in the bottom middle
<p>Prompt 2: Add Examples</p> <p>You are an assistant that extracts the added subject in the edit instruction.</p> <p>Given an edit instruction like “add X to the image”:</p> <ul style="list-style-type: none"> - Extract “X” (the added subject). - Output the extracted subject. - Modify the instruction by replacing “X” with <imagehere> in the original prompt and output the new instruction. <p>Here are some examples:</p> <ol style="list-style-type: none"> 1. add human over the stone in the bottom left → Output: human, add <imagehere> over the stone in the bottom left 2. add a car on the road at the bottom → Output: a car, add <imagehere> on the road at the bottom 3. Add an owl on the left shoulder → Output: an owl, Add <imagehere> on the left shoulder

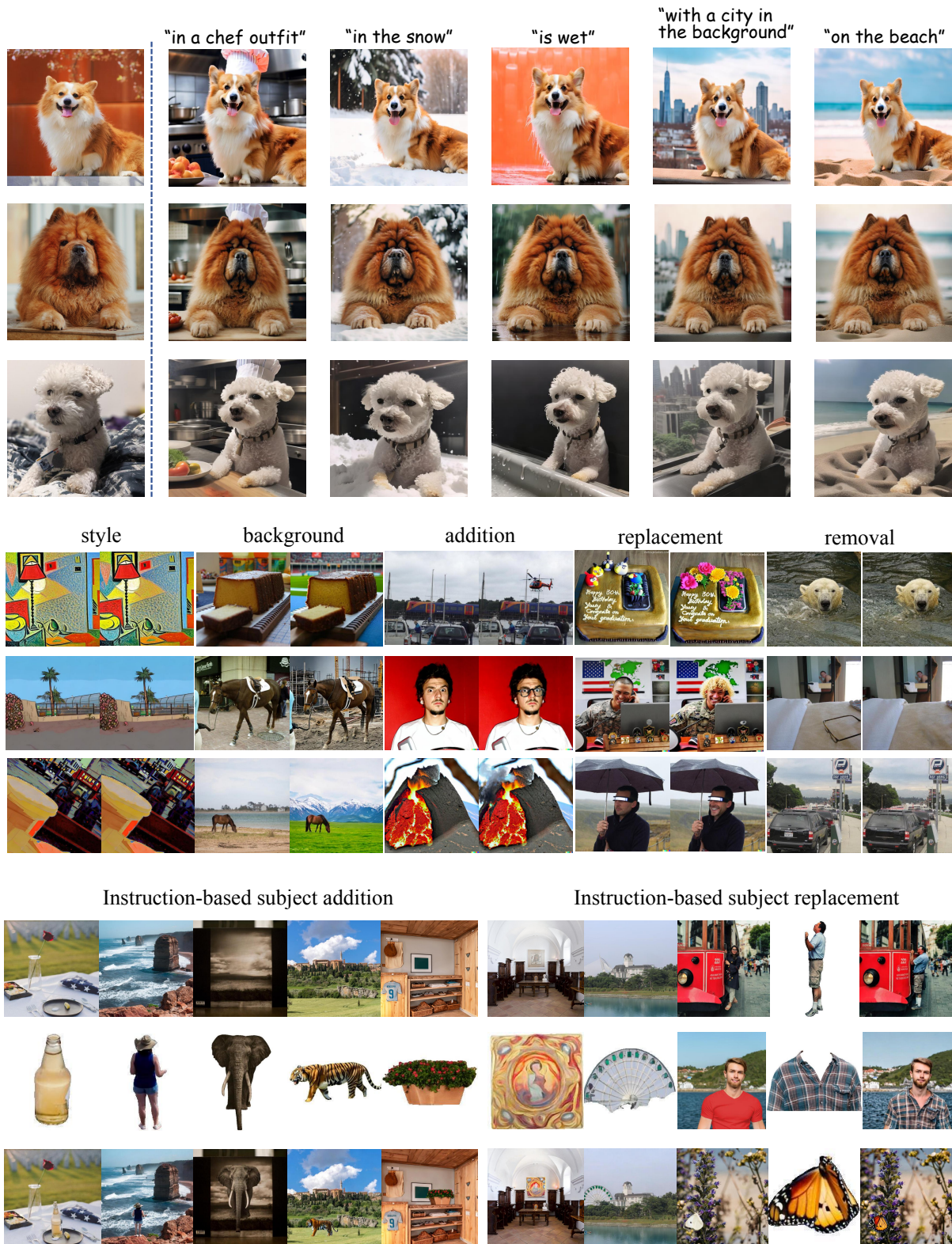


Figure 14: Qualitative results of subject-driven image generation (top), instruction-based image editing (middle), and instruction-based subject-driven image editing (bottom).

Acknowledgments

This work was supported by the National Natural Science Foundation of China (No.62172393), and Major Public Welfare Project of Henan Province (No.201300311200).

References

- [1] Abubakar Abid, Ali Abdalla, Ali Abid, Dawood Khan, Abdulrahman Alfozan, and James Zou. 2019. Gradio: Hassle-Free Sharing and Testing of ML Models in the Wild. *arXiv preprint arXiv:1906.02569* (2019).
- [2] Tim Brooks, Aleksander Holynski, and Alexei A Efros. 2023. Instructpix2pix: Learning to follow image editing instructions. In *Proceedings of the IEEE/CVF Conference on Computer Vision and Pattern Recognition*. 18392–18402.
- [3] Alper Canberk, Maksym Bondarenko, Ege Ozguroglu, Ruoshi Liu, and Carl Vondrick. 2025. EraseDraw: Learning to Insert Objects by Erasing Them from Images. In *European Conference on Computer Vision*. Springer, 144–160.
- [4] Junsong Chen, Jincheng Yu, Chongjian Ge, Lewei Yao, Enze Xie, Yue Wu, Zhongdao Wang, James Kwok, Ping Luo, Huchuan Lu, et al. 2023. Pixart- α : Fast training of diffusion transformer for photorealistic text-to-image synthesis. *arXiv preprint arXiv:2310.00426* (2023).
- [5] Xi Chen, Yutong Feng, Mengting Chen, Yiyang Wang, Shilong Zhang, Yu Liu, Yujun Shen, and Hengshuang Zhao. 2024. Zero-shot image editing with reference imitation. *Advances in Neural Information Processing Systems* 37 (2024), 84010–84032.
- [6] Xi Chen, Lianghua Huang, Yu Liu, Yujun Shen, Deli Zhao, and Hengshuang Zhao. 2024. Anydoor: Zero-shot object-level image customization. In *Proceedings of the IEEE/CVF conference on computer vision and pattern recognition*. 6593–6602.
- [7] Xi Chen, Zhifei Zhang, He Zhang, Yuqian Zhou, Soo Ye Kim, Qing Liu, Yijun Li, Jianming Zhang, Nanxuan Zhao, Yilin Wang, et al. 2024. UniReal: Universal Image Generation and Editing via Learning Real-world Dynamics. *arXiv preprint arXiv:2412.07774* (2024).
- [8] Yisol Choi, Sangkyung Kwak, Kyungmin Lee, Hyungwon Choi, and Jinwoo Shin. 2024. Improving Diffusion Models for Authentic Virtual Try-on in the Wild. *arXiv preprint arXiv:2403.05139* (2024).
- [9] Hyung Won Chung, Le Hou, Shayne Longpre, Barret Zoph, Yi Tay, William Fedus, Yunxuan Li, Xuezhi Wang, Mostafa Dehghani, Siddhartha Brahma, et al. 2024. Scaling instruction-finetuned language models. *Journal of Machine Learning Research* 25, 70 (2024), 1–53.
- [10] Patrick Esser, Sumith Kulal, Andreas Blattmann, Rahim Entezari, Jonas Müller, Harry Saini, Yam Levi, Dominik Lorenz, Axel Sauer, Frederic Boesel, et al. 2024. Scaling rectified flow transformers for high-resolution image synthesis. In *Forty-first International Conference on Machine Learning*.
- [11] Yuxin Fang, Wen Wang, Binhui Xie, Quan Sun, Ledell Wu, Xinggang Wang, Tiejun Huang, Xinlong Wang, and Yue Cao. 2023. Eva: Exploring the limits of masked visual representation learning at scale. In *Proceedings of the IEEE/CVF Conference on Computer Vision and Pattern Recognition*. 19358–19369.
- [12] Tsu-Jui Fu, Wenzhe Hu, Xianzhi Du, William Yang Wang, Yinfei Yang, and Zhe Gan. 2023. Guiding instruction-based image editing via multimodal large language models. *arXiv preprint arXiv:2309.17102* (2023).
- [13] Yuying Ge, Sijie Zhao, Chen Li, Yixiao Ge, and Ying Shan. 2024. SEED-DataEdit Technical Report: A Hybrid Dataset for Instructional Image Editing. *arXiv preprint arXiv:2405.04007* (2024).
- [14] Xavier Glorot, Antoine Bordes, and Yoshua Bengio. 2011. Deep sparse rectifier neural networks. In *Proceedings of the fourteenth international conference on artificial intelligence and statistics*. JMLR Workshop and Conference Proceedings, 315–323.
- [15] Zhen Han, Zeyinzi Jiang, Yulin Pan, Jingfeng Zhang, Chaojie Mao, Chenwei Xie, Yu Liu, and Jingren Zhou. 2024. ACE: All-round Creator and Editor Following Instructions via Diffusion Transformer. *arXiv preprint arXiv:2410.00086* (2024).
- [16] Jixuan He, Wanhua Li, Ye Liu, Junsik Kim, Donglai Wei, and Hanspeter Pfister. 2024. Affordance-Aware Object Insertion via Mask-Aware Dual Diffusion. *arXiv preprint arXiv:2412.14462* (2024).
- [17] Runze He, Kai Ma, Linjiang Huang, Shaofei Huang, Jialin Gao, Xiaoming Wei, Jiao Dai, Jizhong Han, and Si Liu. 2024. Freeedit: Mask-free reference-based image editing with multi-modal instruction. *arXiv preprint arXiv:2409.18071* (2024).
- [18] Teng-Fang Hsiao, Bo-Kai Ruan, Yi-Lun Wu, Tzu-Ling Lin, and Hong-Han Shuai. 2025. TF-TI2I: Training-Free Text-and-Image-to-Image Generation via Multi-Modal Implicit-Context Learning in Text-to-Image Models. *arXiv preprint arXiv:2503.15283* (2025).
- [19] Hexiang Hu, Kelvin CK Chan, Yu-Chuan Su, Wenhui Chen, Yandong Li, Kihyuk Sohn, Yang Zhao, Xue Ben, Boqing Gong, William Cohen, et al. 2024. Instruct-Imagen: Image generation with multi-modal instruction. In *Proceedings of the IEEE/CVF Conference on Computer Vision and Pattern Recognition*. 4754–4763.
- [20] Lianghua Huang, Wei Wang, Zhi-Fan Wu, Huanzhang Dou, Yupeng Shi, Yutong Feng, Chen Liang, Yu Liu, and Jingren Zhou. 2024. Group diffusion transformers are unsupervised multitask learners. (2024).
- [21] Yuzhou Huang, Liangbin Xie, Xintao Wang, Ziyang Yuan, Xiaodong Cun, Yixiao Ge, Jiantao Zhou, Chao Dong, Rui Huang, Ruimao Zhang, et al. 2024. Smartedit: Exploring complex instruction-based image editing with multimodal large language models. In *Proceedings of the IEEE/CVF Conference on Computer Vision and Pattern Recognition*. 8362–8371.
- [22] Zhipeng Huang, Shaobin Zhuang, Canmiao Fu, Binxin Yang, Ying Zhang, Chong Sun, Zhizheng Zhang, Yali Wang, Chen Li, and Zheng-Jun Zha. 2025. WeGen: A Unified Model for Interactive Multimodal Generation as We Chat. *arXiv preprint arXiv:2503.01115* (2025).
- [23] Mude Hui, Siwei Yang, Bingchen Zhao, Yichun Shi, Heng Wang, Peng Wang, Yuyin Zhou, and Cihang Xie. 2024. Hq-edit: A high-quality dataset for instruction-based image editing. *arXiv preprint arXiv:2404.09990* (2024).
- [24] Aaron Hurst, Adam Lerer, Adam P Goucher, Adam Perelman, Aditya Ramesh, Aidan Clark, AJ Ostrow, Akila Welihinda, Alan Hayes, Alec Radford, et al. 2024. Gpt-4o system card. *arXiv preprint arXiv:2410.21276* (2024).
- [25] Hao Kang, Stathi Fotiadis, Liming Jiang, Qing Yan, Yumin Jia, Zichuan Liu, Min Jin Chong, and Xin Lu. 2025. Flux Already Knows—Activating Subject-Driven Image Generation without Training. *arXiv preprint arXiv:2504.11478* (2025).
- [26] Taewook Kim, Wei Chen, and Qiang Qiu. 2024. Learning to Customize Text-to-Image Diffusion In Diverse Context. *arXiv preprint arXiv:2410.10058* (2024).
- [27] Diederik P Kingma. 2013. Auto-encoding variational bayes. *arXiv preprint arXiv:1312.6114* (2013).
- [28] Alexander Kirillov, Eric Mintun, Nikhila Ravi, Hanzi Mao, Chloe Rolland, Laura Gustafson, Tete Xiao, Spencer Whitehead, Alexander C Berg, Wan-Yen Lo, et al. 2023. Segment anything. In *Proceedings of the IEEE/CVF International Conference on Computer Vision*. 4015–4026.
- [29] Black Forest Labs. 2023. FLUX. <https://github.com/black-forest-labs/flux>.
- [30] Duong H Le, Tuan Pham, Sangho Lee, Christopher Clark, Aniruddha Kembhavi, Stephan Mandt, Ranjay Krishna, and Jiasen Lu. 2024. One Diffusion to Generate Them All. *arXiv preprint arXiv:2411.16318* (2024).
- [31] Dongxu Li, Junnan Li, and Steven Hoi. 2024. Blip-diffusion: Pre-trained subject representation for controllable text-to-image generation and editing. *Advances in Neural Information Processing Systems* 36 (2024).
- [32] Junnan Li, Dongxu Li, Silvio Savarese, and Steven Hoi. 2023. Blip-2: Bootstrapping language-image pre-training with frozen image encoders and large language models. In *International conference on machine learning*. PMLR, 19730–19742.
- [33] Pengzhi Li, Qiang Nie, Ying Chen, Xi Jiang, Kai Wu, Yuhuan Lin, Yong Liu, Jinlong Peng, Chengjie Wang, and Feng Zheng. 2025. Tuning-free image customization with image and text guidance. In *European Conference on Computer Vision*. Springer, 233–250.
- [34] Tianle Li, Max Ku, Cong Wei, and Wenhui Chen. 2023. Dreamedit: Subject-driven image editing. *arXiv preprint arXiv:2306.12624* (2023).
- [35] Wei Li, Xue Xu, Jiachen Liu, and Xinyan Xiao. 2024. UNIMO-G: Unified Image Generation through Multimodal Conditional Diffusion. In *Proceedings of the 62nd Annual Meeting of the Association for Computational Linguistics (Volume 1: Long Papers)*, Lun-Wei Ku, Andre Martins, and Vivek Srikumar (Eds.). Association for Computational Linguistics, Bangkok, Thailand, 6173–6188. doi:10.18653/v1/2024.acl-long.335
- [36] Wentong Li, Yuqian Yuan, Jian Liu, Dongqi Tang, Song Wang, Jie Qin, Jianke Zhu, and Lei Zhang. 2024. Tokenpacker: Efficient visual projector for multimodal llm. *arXiv preprint arXiv:2407.02392* (2024).
- [37] Yaowei Li, Lingling Li, Zhaoyang Zhang, Xiaoyu Li, Guangzhi Wang, Hongxiang Li, Xiaodong Cun, Ying Shan, and Yuexian Zou. 2025. Blobctrl: A unified and flexible framework for element-level image generation and editing. *arXiv preprint arXiv:2503.13434* (2025).
- [38] Zhaowei Li, Wei Wang, YiQing Cai, Xu Qi, Pengyu Wang, Dong Zhang, Hang Song, Botian Jiang, Zhida Huang, and Tao Wang. 2024. Unifiedmllm: Enabling unified representation for multi-modal multi-tasks with large language model. *arXiv preprint arXiv:2408.02503* (2024).
- [39] Zhong-Yu Li, Ruoyi Du, Juncheng Yan, Le Zhuo, Zhen Li, Peng Gao, Zhanyu Ma, and Ming-Ming Cheng. 2025. VisualCloze: A Universal Image Generation Framework via Visual In-Context Learning. *arXiv preprint arXiv:2504.07960* (2025).
- [40] Chen Liang, Lianghua Huang, Jingwu Fang, Huanzhang Dou, Wei Wang, Zhi-Fan Wu, Yupeng Shi, Junge Zhang, Xin Zhao, and Yu Liu. 2025. IDEA-Bench: How Far are Generative Models from Professional Designing?. In *Proceedings of the Computer Vision and Pattern Recognition Conference*. 18541–18551.
- [41] Weifeng Lin, Xinyu Wei, Renrui Zhang, Le Zhuo, Shitian Zhao, Siyuan Huang, Junlin Xie, Yu Qiao, Peng Gao, and Hongsheng Li. 2024. PixWizard: Versatile image-to-image visual assistant with open-language instructions. *arXiv preprint arXiv:2409.15278* (2024).
- [42] Yijing Lin, Mengqi Huang, Shuhan Zhuang, and Zhendong Mao. 2025. RealGeneral: Unifying Visual Generation via Temporal In-Context Learning with Video Models. *arXiv preprint arXiv:2503.10406* (2025).
- [43] Shilong Liu, Zhaoyang Zeng, Tianhe Ren, Feng Li, Hao Zhang, Jie Yang, Qing Jiang, Chunyuan Li, Jianwei Yang, Hang Su, et al. 2025. Grounding dino: Marrying dino with grounded pre-training for open-set object detection. In *European Conference on Computer Vision*. Springer, 38–55.

- [44] I Loshchilov. 2017. Decoupled weight decay regularization. *arXiv preprint arXiv:1711.05101* (2017).
- [45] Xichen Pan, Li Dong, Shaohan Huang, Zhiliang Peng, Wenhui Chen, and Furu Wei. 2023. Kosmos-g: Generating images in context with multimodal large language models. *arXiv preprint arXiv:2310.02992* (2023).
- [46] William Peebles and Saining Xie. 2023. Scalable diffusion models with transformers. In *Proceedings of the IEEE/CVF International Conference on Computer Vision*. 4195–4205.
- [47] Yuan Peng, Yuxin Cui, Haomiao Tang, Zekun Qi, Runpei Dong, Jing Bai, Chunrui Han, Zheng Ge, Xiangyu Zhang, and Shu-Tao Xia. 2024. Dreambench++: A human-aligned benchmark for personalized image generation. *arXiv preprint arXiv:2406.16855* (2024).
- [48] Alec Radford, Jong Wook Kim, Chris Hallacy, Aditya Ramesh, Gabriel Goh, Sandhini Agarwal, Girish Sastry, Amanda Askell, Pamela Mishkin, Jack Clark, et al. 2021. Learning transferable visual models from natural language supervision. In *International conference on machine learning*. PMLR, 8748–8763.
- [49] Tianhe Ren, Shilong Liu, Ailing Zeng, Jing Lin, Kunchang Li, He Cao, Jiayu Chen, Xinyu Huang, Yukang Chen, Feng Yan, et al. 2024. Grounded sam: Assembling open-world models for diverse visual tasks. *arXiv preprint arXiv:2401.14159* (2024).
- [50] Robin Rombach, Andreas Blattmann, Dominik Lorenz, Patrick Esser, and Björn Ommer. 2022. High-resolution image synthesis with latent diffusion models. In *Proceedings of the IEEE/CVF conference on computer vision and pattern recognition*. 10684–10695.
- [51] Nataniel Ruiz, Yuanzhen Li, Varun Jampani, Yael Pritch, Michael Rubinstein, and Kfir Aberman. 2023. Dreambooth: Fine tuning text-to-image diffusion models for subject-driven generation. In *Proceedings of the IEEE/CVF conference on computer vision and pattern recognition*. 22500–22510.
- [52] Shelly Sheynin, Adam Polyak, Uriel Singer, Yuval Kirstain, Amit Zohar, Oron Ashual, Devi Parikh, and Yaniv Taigman. 2024. Emu edit: Precise image editing via recognition and generation tasks. In *Proceedings of the IEEE/CVF Conference on Computer Vision and Pattern Recognition*. 8871–8879.
- [53] Jing Shi, Ning Xu, Trung Bui, Franck Deroncourt, Zheng Wen, and Chenliang Xu. 2020. A benchmark and baseline for language-driven image editing. In *Proceedings of the Asian Conference on Computer Vision*.
- [54] Quan Sun, Yufeng Cui, Xiaosong Zhang, Fan Zhang, Qiying Yu, Yuezhe Wang, Yongming Rao, Jingjing Liu, Tiejun Huang, and Xinlong Wang. 2024. Generative multimodal models are in-context learners. In *Proceedings of the IEEE/CVF Conference on Computer Vision and Pattern Recognition*. 14398–14409.
- [55] Roman Suvorov, Elizaveta Logacheva, Anton Mashikhin, Anastasia Remizova, Arsenii Ashukha, Aleksei Silvestrov, Naejin Kong, Harshith Goka, Kiwoong Park, and Victor Lempitsky. 2022. Resolution-robust large mask inpainting with fourier convolutions. In *Proceedings of the IEEE/CVF winter conference on applications of computer vision*. 2149–2159.
- [56] Zhenxiong Tan, Songhua Liu, Xingyi Yang, Qiaochu Xue, and Xinchao Wang. 2024. Ominicontrol: Minimal and universal control for diffusion transformer. *arXiv preprint arXiv:2411.15098* 3 (2024).
- [57] Ming Tao, Bing-Kun Bao, Yaowei Wang, and Changsheng Xu. 2024. Do We Need to Design Specific Diffusion Models for Different Tasks? Try ONE-PIC. *arXiv preprint arXiv:2412.05619* (2024).
- [58] MosaicML NLP Team et al. 2023. Introducing mpt-7b: A new standard for open-source, commercially usable llms.
- [59] Qwen Team. 2024. Qwen2.5: A Party of Foundation Models. <https://qwenlm.github.io/blog/qwen2.5/>
- [60] Peng Wang, Shuai Bai, Sinan Tan, Shijie Wang, Zhihao Fan, Jinze Bai, Keqin Chen, Xuejing Liu, Jialin Wang, Wenbin Ge, Yang Fan, Kai Dang, Mengfei Du, Xuancheng Ren, Rui Men, Dayiheng Liu, Chang Zhou, Jingren Zhou, and Junyang Lin. 2024. Qwen2-VL: Enhancing Vision-Language Model's Perception of the World at Any Resolution. *arXiv preprint arXiv:2409.12191* (2024).
- [61] Feize Wu, Yun Pang, Junyi Zhang, Lianyu Pang, Jian Yin, Baoquan Zhao, Qing Li, and Xudong Mao. 2025. Core: Context-regularized text embedding learning for text-to-image personalization. In *Proceedings of the AAAI Conference on Artificial Intelligence*, Vol. 39. 8377–8385.
- [62] Shitao Xiao, Yuezhe Wang, Junjie Zhou, Huaying Yuan, Xingrun Xing, Ruirui Yan, Shutong Wang, Tiejun Huang, and Zheng Liu. 2024. Omnigen: Unified image generation. *arXiv preprint arXiv:2409.11340* (2024).
- [63] Yingjing Xu, Jie Kong, Jiazhi Wang, Xiao Pan, Bo Lin, and Qiang Liu. 2024. InsightEdit: Towards Better Instruction Following for Image Editing. *arXiv preprint arXiv:2411.17323* (2024).
- [64] Le Xue, Manli Shu, Anas Awadalla, Jun Wang, An Yan, Senthil Purushwalkam, Honglu Zhou, Viraj Prabhu, Yutong Dai, Michael S Ryoo, et al. 2024. xgen-mm (blip-3): A family of open large multimodal models. *arXiv preprint arXiv:2408.08872* (2024).
- [65] Binxin Yang, Shuyang Gu, Bo Zhang, Ting Zhang, Xuejin Chen, Xiaoyan Sun, Dong Chen, and Fang Wen. 2023. Paint by example: Exemplar-based image editing with diffusion models. In *Proceedings of the IEEE/CVF Conference on Computer Vision and Pattern Recognition*. 18381–18391.
- [66] Yicheng Yang, Pengxiang Li, Lu Zhang, Liqian Ma, Ping Hu, Siyu Du, Yunzhi Zhuge, Xu Jia, and Huchuan Lu. 2024. DreamMix: Decoupling Object Attributes for Enhanced Editability in Customized Image Inpainting. *arXiv preprint arXiv:2411.17223* (2024).
- [67] Hu Ye, Jun Zhang, Sibao Liu, Xiao Han, and Wei Yang. 2023. Ip-adapter: Text compatible image prompt adapter for text-to-image diffusion models. *arXiv preprint arXiv:2308.06721* (2023).
- [68] Ahmet Burak Yildirim, Vedat Baday, Erkut Erdem, Aykut Erdem, and Aysegül Dundar. 2023. Inst-inpaint: Instructing to remove objects with diffusion models. *arXiv preprint arXiv:2304.03246* (2023).
- [69] Qifan Yu, Wei Chow, Zhongqi Yue, Kaihang Pan, Yang Wu, Xiaoyang Wan, Juncheng Li, Siliang Tang, Hanwang Zhang, and Yueting Zhuang. 2024. AnyEdit: Mastering Unified High-Quality Image Editing for Any Idea. *arXiv preprint arXiv:2411.15738* (2024).
- [70] Kai Zhang, Lingbo Mo, Wenhui Chen, Huan Sun, and Yu Su. 2024. Magicbrush: A manually annotated dataset for instruction-guided image editing. *Advances in Neural Information Processing Systems* 36 (2024).
- [71] Haozhe Zhao, Xiaojian Ma, Liang Chen, Shuzheng Si, Rujie Wu, Kaikai An, Peiyu Yu, Minjia Zhang, Qing Li, and Baobao Chang. 2024. UltraEdit: Instruction-based Fine-Grained Image Editing at Scale. *arXiv preprint arXiv:2407.05282* (2024).
- [72] Jun Zhou, Jiahao Li, Zunnan Xu, Hanhui Li, Yiji Cheng, Fa-Ting Hong, Qin Lin, Qinglin Lu, and Xiaodan Liang. 2025. FireEdit: Fine-grained Instruction-based Image Editing via Region-aware Vision Language Model. *arXiv preprint arXiv:2503.19839* (2025).